

Heavy quark production as sensitive test for an improved description of high energy hadron collisions

Ph. Hägler¹, R. Kirschner², A. Schäfer¹, L. Szymanowski^{1,3}, O.V. Teryaev^{1,4}

¹Institut für Theoretische Physik, Universität Regensburg, D-93040 Regensburg, Germany

²Institut für Theoretische Physik, Universität Leipzig, D-04109 Leipzig, Germany

³Soltan Institute for Nuclear Studies, Hoza 69, 00681 Warsaw, Poland

⁴Bogoliubov Laboratory of Theoretical Physics, JINR, 141980 Dubna, Russia

QCD dynamics at small quark and gluon momentum fractions or large total energy, which plays a major role for HERA, the Tevatron, RHIC and LHC physics, is still poorly understood. For one of the simplest processes, namely $b\bar{b}$ production, next-to-leading-order perturbation theory fails. We show that the combination of two recently developed theoretical concepts, the k_\perp -factorization and the next-to-leading-logarithmic-approximation BFKL vertex, gives perfect agreement with data. One can therefore hope that these concepts provide a valuable foundation for the description of other high energy processes.

Existing QCD calculations describe many high energy observables which involve partonic transverse momentum rather poorly. This is also true for the theoretically especially clean case of $b\bar{b}$ production, which was investigated experimentally at Fermilab [1]. Since central quark-antiquark production at $\sqrt{s} = 1.8$ TeV is sensitive to very small gluon momentum fraction $x \approx 10^{-2} - 10^{-4}$, one probes the gluon content of the nucleon at small x , which is a central issue of current research. We reconsider this process and combine as essential new ingredients the k_t -factorization scheme with the next-to-leading-logarithmic-approximation (NLLA) BFKL production vertex derived in [2]. The k_t -factorization approach for the description of high energy processes [3–6] differs strongly from the conventional NLO collinear approximation (e.g. [7]) because it takes the non-vanishing transverse momenta of the scattering partons into account. The usual gluon densities are replaced by unintegrated gluon distributions which depend on the transverse momentum k_t . These together with the k_t -factorization form a basis for a general calculation scheme for high energy (i.e. small x). The standard collinear approximation has the advantage of being closely related to the operator product expansion. It is, however, only justified for the processes dominated by $x = \mathcal{O}(1)$. In application to processes governed by small x the k_t -factorization approach has the advantage that its approximations correspond to the dominant kinematics. Essential small x contributions are included in the Born approximation which in the collinear approach are accounted for in higher orders only. This is well known from the case of structure functions where the DGLAP evolution is appropriate for $x = \mathcal{O}(1)$ and the BFKL evolution for small x .

While the k_t -factorization formalism is very attractive theoretically, its phenomenological usefulness has been

mostly tested in the case of the structure function F_2 [9,10]. The NLLA BFKL vertices are just the ones needed to treat semi-hard central production at collider energies in this approach.

In our calculation we use one particular element of the NLLA BFKL formalism [2,8], namely the effective vertex for quark-antiquark production. Thus our calculation can be seen as a first phenomenological application of this vertex which decides whether the NLLA BFKL formalism can be hoped to converge.

One special aspect of the reaction we investigate is the possible loss of gauge invariance when a $q\bar{q}$ production vertex is incorporated into an amplitude with off-shell gluons. In the BFKL approach, however, gauge invariance is ensured automatically by the use of the just mentioned NLL effective vertex which is valid in quasi multi Regge kinematics (QMRK), i.e. when the q and \bar{q} have similar rapidities and form a cluster (in contrast to LLA, where the particles are produced with a large rapidity gap).

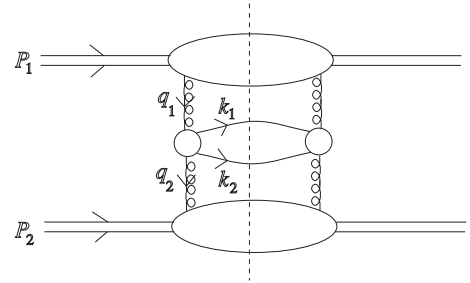


FIG. 1. The basic diagram

We begin with the following definition for the light cone coordinates and the momenta of the scattering hadrons in the c.m. frame

$$k^+ = k^0 + k^3, \quad k^- = k^0 - k^3, \quad k_\perp = (0, k^1, k^2, 0) = (0, \mathbf{k}, 0), \\ P_1^+ = P_2^- = \sqrt{s}, \quad P_1^- = P_2^+ = 0, \quad P_{1\perp} = P_{2\perp} = 0.$$

The Mandelstam variable s is as usual the c.m. energy squared. As defined in fig. 1, q_1 and q_2 are the momenta of the gluons and the on-shell quark and antiquark have momentum k_1 respectively k_2 . In the high energy (large s) regime we have

$$k_1^+ + k_2^+ = q_1^+ - q_2^+ \approx q_1^+,$$

$$\begin{aligned} k_1^- + k_2^- &= q_1^- - q_2^- \approx -q_2^-, \\ q_1^2 &\approx q_{1\perp}^2, q_2^2 \approx q_{2\perp}^2. \end{aligned}$$

The longitudinal momentum fractions of the gluons are $x_1 = q_1^+/P_1^+$, $x_2 = -q_2^-/P_2^-$.

The cross section for heavy quark pair production in the k_t -factorization approach is then given by [3,4]

$$\begin{aligned} \sigma_{P_1 P_2 \rightarrow q \bar{q} X} &= \frac{1}{16(2\pi)^4} \int \frac{d^3 k_1}{k_1^+} \frac{d^3 k_2}{k_2^+} d^2 q_{1\perp} d^2 q_{2\perp} \\ &\delta^2(q_{1\perp} - q_{2\perp} - k_{1\perp} - k_{2\perp}) \mathcal{F}(x_1, q_{1\perp}) \frac{1}{(q_{1\perp}^2)^2} \\ &\left\{ \frac{\psi^{\dagger c_2 c_1} \psi^{c_2 c_1}}{(N^2 - 1)^2} \right\} \frac{1}{(q_{2\perp}^2)^2} \mathcal{F}(x_2, q_{2\perp}). \end{aligned} \quad (1)$$

The factor $(N^2 - 1)^2$ reflects the projection on color singlet, where N is the number of colors. The hard amplitude $\psi^{c_2 c_1}(x_1, x_2, q_{1\perp}, q_{2\perp}, k_1, k_2)$ is calculable in perturbation theory, whereas the unintegrated gluon distribution $\mathcal{F}(x, q_\perp)$ has to be measured or modelled. We choose the argument μ^2 of the strong coupling constant $\alpha_S(\mu^2)$ in the hard amplitude $\psi^{c_2 c_1}$ to be equal to $\mathbf{q}_1^2 = -q_{1\perp}^2$ respectively $\mathbf{q}_2^2 = -q_{2\perp}^2$ [11].

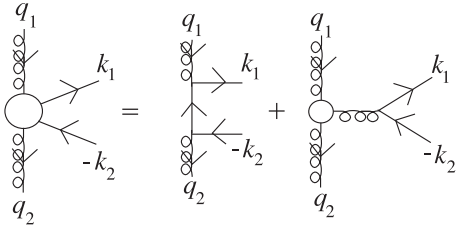


FIG. 2. The effective vertex

We generalize the results on the $q\bar{q}$ production vertex presented in [2] for massless QCD in an obvious way in order to take the masses m of the produced quarks into account. The resulting vertex $\Psi^{c_2 c_1}$ is given by a sum of two terms

$$\Psi^{c_2 c_1} = -g^2 (t^{c_1} t^{c_2} b(k_1, k_2) - t^{c_2} t^{c_1} b^T(k_2, k_1)), \quad (2)$$

where t^c are the colour group generators in the fundamental representation. The connection between $\psi^{c_2 c_1}$ in eq. (1) and $\Psi^{c_2 c_1}$ in eq. (2) is given by

$$\psi^{c_2 c_1} = \bar{u}(k_1) \Psi^{c_2 c_1} v(k_2),$$

with the on-shell quark and antiquark spinors $u(k)$ and $v(k)$. The expression for $b(k_1, k_2)$ is a sum of two terms

$$b(k_1, k_2) = \gamma^- \frac{\not{q}_{1\perp} - \not{k}_{1\perp} - m}{(q_1 - k_1)^2 - m^2} \gamma^+ - \frac{\gamma_\beta \Gamma^{+\beta}(q_2, q_1)}{(k_1 + k_2)^2}, \quad (3)$$

The first term on the r.h.s. of eq. (3) describes the production of a $q\bar{q}$ pair by means of usual vertices (see fig. 2),

the second term involves the light-cone projection of the effective vertex $\Gamma^{+\beta}(q_2, q_1)$, which describes the transition of two t -channel gluons (reggeons) with momenta q_1 and q_2 to a gluon with momentum $k_1 + k_2$

$$\begin{aligned} \Gamma^{+\beta}(q_2, q_1) &= 2(q_1 + q_2)^\beta - 2q_1^+ n^{-\beta} - 2q_2^- n^{+\beta} \\ &\quad - 2t_1 \frac{n^{-\beta}}{q_1^- - q_2^-} + 2t_2 \frac{n^{+\beta}}{q_1^+ - q_2^+}, \end{aligned} \quad (4)$$

with $t_{1/2} = q_{1/2}^2$. This effective vertex differs from the usual triple-gluon vertex by the appearance of the last two terms. They are related to Feynman diagrams in which the $q\bar{q}$ pair is not produced by the t -channel gluons but in other ways. These two last terms in eq. (4) are also required by gauge invariance, $\Gamma^{+\beta}(q_2, q_1)(q_1 - q_2)_\beta = 0$. Another consequence of gauge invariance is the vanishing of the matrix element of the effective vertex $\Psi^{c_2 c_1}$ between on-mass-shell quark and antiquark states in the limit of small $q_{1\perp}$ or $q_{2\perp}$

$$\bar{u}(k_1) \Psi^{c_2 c_1} v(k_2) \rightarrow 0 \quad \text{for } q_{1\perp} \text{ or } q_{2\perp} \rightarrow 0.$$

The function $b^T(k_2, k_1)$ is very similar to (3)

$$b^T(k_2, k_1) = \gamma^+ \frac{\not{q}_{1\perp} - \not{k}_{2\perp} + m}{(q_1 - k_2)^2 - m^2} \gamma^- - \frac{\gamma_\beta \Gamma^{+\beta}(q_2, q_1)}{(k_1 + k_2)^2}.$$

The unintegrated gluon distribution is related to the standard gluon distribution by

$$xg(x, \mathbf{q}^2) = \int_0^\infty \frac{d\mathbf{k}^2}{\mathbf{k}^2} \Theta(\mathbf{q}^2 - \mathbf{k}^2) \mathcal{F}(x, \mathbf{k}).$$

Taking the derivative of this expression makes it obvious that $\mathcal{F}(x, \mathbf{k})$ includes the evolution of $xg(x, \mathbf{q}^2)$, which is given by the BFKL and/or DGLAP equation. Since the unintegrated gluon distribution is not known at small \mathbf{k} , we write this equation as

$$xg(x, \mathbf{q}^2) = xg(x, q_0^2) + \int_{q_0^2}^\infty \frac{d\mathbf{k}^2}{\mathbf{k}^2} \Theta(\mathbf{q}^2 - \mathbf{k}^2) \mathcal{F}(x, \mathbf{k}). \quad (5)$$

This formula has been repeatedly used [12,13,4,14] and introduces the a priori unknown initial scale q_0 and the initial gluon distribution $xg(x, q_0^2)$. Following [10], one may neglect the hard cross section dependence on \mathbf{q} in the soft region $|\mathbf{q}| < q_0$, so that

$$\begin{aligned} \frac{1}{q_{1\perp}^2} \left\{ \frac{\psi^{\dagger c_2 c_1} \psi^{c_2 c_1}}{(N^2 - 1)^2} \right\} \frac{1}{q_{2\perp}^2} &\equiv S(q_{1\perp}, q_{2\perp}) \rightarrow \\ &S(q_{1\perp}, q_{2\perp}) \Theta(\mathbf{q}_1^2 - q_0^2) \Theta(\mathbf{q}_2^2 - q_0^2) \\ &+ S(q_{1\perp}, 0) \Theta(\mathbf{q}_1^2 - q_0^2) \Theta(q_0^2 - \mathbf{q}_2^2) \\ &+ S(0, q_{2\perp}) \Theta(\mathbf{q}_2^2 - q_0^2) \Theta(q_0^2 - \mathbf{q}_1^2) \\ &+ S(0, 0) \Theta(q_0^2 - \mathbf{q}_1^2) \Theta(q_0^2 - \mathbf{q}_2^2). \end{aligned} \quad (6)$$

Note that the very existence of the finite limit $q_\perp \rightarrow 0$ follows from the decrease of the production amplitude

due to gauge invariance. Substituting this formula in (1) using eq. (5) one may easily perform the integration over q_{\perp} . As a result, $S(0,0)$ produces the standard expression of collinear factorization (ref. [10,14]), while $S(q_{1\perp},0)$, $S(0,q_{2\perp})$ correspond to the asymmetric configurations, where one of the gluons is described by the unintegrated distribution and the other by the integrated one. Here it is important to notice that when we insert (5), (6) in (1) the coupling constant α_s in the term proportional to $xg(x, q_0^2)$ is taken to be $\alpha_s(q_0^2)$.

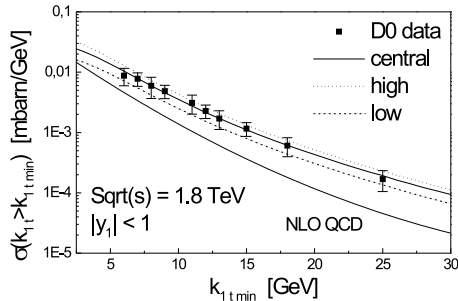


FIG. 3. The calculated b cross section in comparison to experimental data from the D0 Collaboration and the NLO QCD result with MRSR2 structure functions and $m_b = 4.75$ GeV from [15]

In all our numerical calculations we used for the unintegrated gluon distribution $\mathcal{F}(x, \mathbf{k})$ the code by Kwiecinski, Martin and Staśto [10], because they use a combination of DGLAP and BFKL equations which governs simultaneously the evolution in Q^2 and x . They obtain an excellent description of $F_2(x, Q^2)$ in a very large x - Q^2 -window. According to our knowledge this is the only unintegrated gluon distribution which has given such a satisfactory result, which justifies our choice. As in the case of the usual gluon distribution function one has to choose an initial scale and an initial distribution function which in the case of [10] are given by

$$q_0^2 = 1 \text{ GeV}^2, \quad xg(x, q_0^2) = 1.57(1-x)^{2.5}. \quad (7)$$

We use these values, which are fixed by the fit to $F_2(x, Q^2)$, in our calculation.

We consider the production of $b\bar{b}$ -pairs. For the computation we use eqs. (1) and (6) with the unintegrated gluon distribution from [10] and the corresponding values (7). The rapidities and the transverse masses of the produced quark and antiquark are defined by

$$y_{1/2} = \frac{1}{2} \ln\left(\frac{k_{1/2}^+}{k_{1/2}^-}\right), \quad m_{1/2\perp} = \sqrt{m^2 - k_{1/2\perp}^2}.$$

The Bjorken-variables of the gluons can then be written as

$$x_1 = \frac{1}{\sqrt{s}}(m_{1\perp}e^{y_1} + m_{2\perp}e^{y_2}),$$

$$x_2 = \frac{1}{\sqrt{s}}(m_{1\perp}e^{-y_1} + m_{2\perp}e^{-y_2}).$$

In fig. 3 we show our results for inclusive b production, together with experimental results measured by the D0 Collaboration [16] (see Table II) in $\sqrt{s} = 1.8$ TeV $p\bar{p}$ collisions. We obtain this cross section by integrating out all antibottom variables in eq. (1).

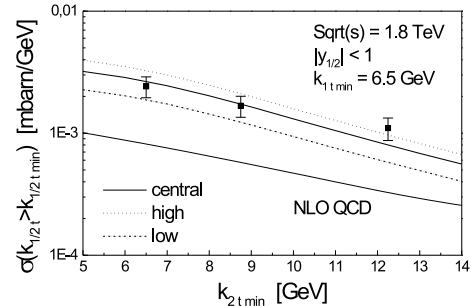


FIG. 4. The result for the semi differential $b\bar{b}$ cross section at $k_{1\perp min} = 6.5$ GeV, compared to CDF data and the NLO QCD result with MRSD0 structure functions and $m_b = 4.75$ GeV from [1]

The variable $k_{1\perp min}$ is the lower integration cut on the transverse momentum of the produced b quark. To get an indication of the theoretical uncertainties apart from higher order contributions which are not available at the moment we proceed in a similar way as the authors of ref. [1] and present our calculations for three different choices of Λ_{QCD} and the bottom quark mass

$$\begin{aligned} \text{high} &: \Lambda^{(5)} = 180 \text{ MeV}, \quad m_b = 4.5 \text{ GeV}, \\ \text{central} &: \Lambda^{(5)} = 150 \text{ MeV}, \quad m_b = 4.7 \text{ GeV}, \\ \text{low} &: \Lambda^{(5)} = 100 \text{ MeV}, \quad m_b = 4.9 \text{ GeV}, \end{aligned}$$

Our result is in very good quantitative agreement with data over the whole range of $k_{1\perp min}$. The corresponding central QCD NLO calculation has a similar shape, but is about a factor of 2 – 3 smaller than our central result (see for example fig. 11 in [15]).

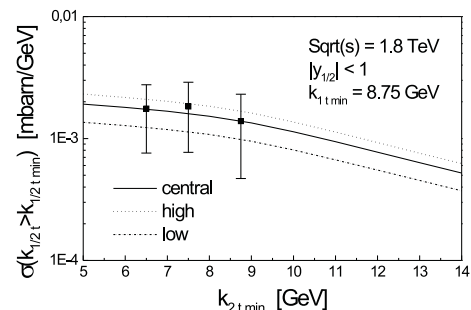


FIG. 5. The result for the semi differential $b\bar{b}$ cross section at $k_{1\perp min} = 8.75$ GeV, compared to CDF data

We now turn to $b\bar{b}$ correlations in $\sqrt{s} = 1.8$ TeV $p\bar{p}$ collisions, which have been measured by the CDF collaboration at Fermilab [1]. The correlations of the quark and antiquark give an insight into the dynamics of the production mechanism and are important in order to study

the limits of the collinear ($k_{1\perp} = -k_{2\perp}$) LO QCD approximation. We present a comparison between our results and the experimental data in fig. 4 and fig. 5. The data points and uncertainties were taken from [1,17]. We find good agreement with experiment for both $k_{1\perp\min} = 6.5$ GeV (fig. 4) and $k_{1\perp\min} = 8.75$ GeV (fig. 5). In this case QCD NLO calculations underestimate the measured cross section roughly by factor of 3 (compare with fig.6 in [1]).

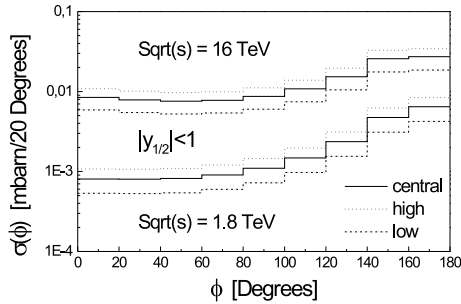


FIG. 6. ϕ distribution of $b\bar{b}$ hadroproduction

An interesting parameter concerning the correlation is the opening angle ϕ between the momentum vectors of the produced quarks in the plane transverse to the beam axis. Our predictions for the corresponding differential cross sections at Fermilab and LHC energies are shown in fig. 6. As expected we find a peak at $\phi = 180^\circ$ which shows the dominance of the collinear part.

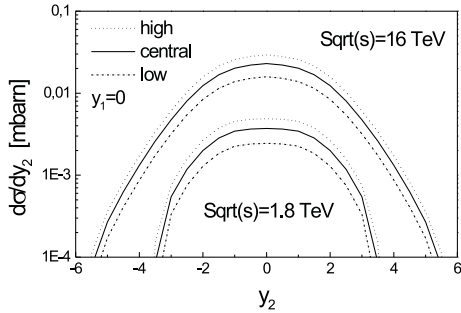


FIG. 7. Rapidity distributions of $b\bar{b}$ hadroproduction

Additionally we present our predictions for rapidity distributions of the \bar{b} for the rapidity of the b being 0 and $\sqrt{s} = 1.8$ TeV respectively $\sqrt{s} = 16$ TeV in fig. 7. Our cross section for $\sqrt{s} = 1.8$ TeV at $y_2 = 0$ is about a factor of 3 larger than the corresponding QCD NLO result from [18].

Let us conclude. We have studied quark-antiquark hadroproduction within the k_t -factorization approach using an unintegrated gluon distribution and a specific effective BFKL vertex for $q\bar{q}$ production. We found very good agreement with experiment for both single b production and $b\bar{b}$ correlations at $\sqrt{s} = 1.8$ TeV. Our approach leads to nontrivial $b\bar{b}$ correlations already at LO perturbation theory, whereas traditional collinear factor-

ization gives them only at NLO and beyond. In contrast, the available NLO calculations [18] are not in agreement with the Tevatron data we compare with [1,17,16].

Our results show that at least those features of the effective $q\bar{q}$ vertex which we tested provide a substantial improvement with respect to the standard collinear treatment.

If further tests of other observables should be equally successful, the NLL BFKL vertices will also allow for a much improved description of many processes to be studied at RHIC and LHC.

We thank J. Kwiecinski, A. Martin and A. Stařto for supplying us with their code for the calculation of the unintegrated gluon distribution.

L. S. would like to acknowledge the support by the DFG.

-
- [1] F. Abe et al., Phys.Rev. D55 (1997) 2546
 - [2] V.S. Fadin and L.N. Lipatov, Nucl. Phys. B477(1996) 767
 - [3] S. Catani, M. Ciafaloni and F. Hautmann, Phys. Lett. B242(1990) 97; Nucl. Phys. B366(1991) 135
 - [4] J.C. Collins and R.K. Ellis, Nucl. Phys. B360(1991) 3
 - [5] G. Camici and M. Ciafaloni, Phys. Lett. B386(1996)341; Nucl. Phys. B496(1997) 305
 - [6] M.G. Ryskin, A.G. Shuvaev and Yu.M. Shabelski, hep-ph/9907507
 - [7] J.C. Collins, D.E. Soper and G. Sterman, Nucl. Phys. B308(1988)833
 - [8] V. Fadin, "BFKL News", Talk given at "LISHEP98", LAFEX school on high energy physics, February 14-21, Rio de Janeiro, Brazil, 1998, hep-ph/9807528
 - [9] I. Bojak and M. Ernst, Phys.Rev. D53 (1996) 80
 - [10] J. Kwiecinski, A. Martin and A. Stařto, Phys.Rev. D56(1997) 3991
 - [11] E.M. Levin, M.G. Ryskin, Yu.M. Shabelski, A.G. Shuvaev, Yad.Fiz. 54 (1991) 1420
 - [12] J. Kwiecinski, Z.Phys. C29(1985) 561
 - [13] M.G. Ryskin and Yu.M. Shabelski, Z.Phys. C61(1994) 517
 - [14] M.G. Ryskin, Yu.M. Shabelski and A.G. Shuvaev, Z.Phys. C69 (1996) 269
 - [15] P. Nason, G. Ridolfi, O. Schneider, G.F. Tartarelli, P. Vikas et al, hep-ph/0003142
 - [16] B. Abbott, D0 Collaboration, FERMILAB-PUB-99-144-E, submitted to Phys.Rev.Lett.
 - [17] F. Abe, CDF collaboration, FERMILAB-PUB-94-131-E
 - [18] M. Mangano, P. Nason, G. Ridolfi, Nucl.Phys. B373 (1992) 295